Article

Journal of
Nanoscience and Nanotechnology
Vol. 14, 1–6, 2014
www.aspbs.com/jnn

Three-Dimensional Numerical Simulation of Vesicle Dynamics in Microscale Shear Flows

Zheng-Yuan Luo[1,2], Long He[1,2], Feng Xu[2,3], and Bo-Feng Bai[1,*]

[1] *State Key Laboratory of Multiphase Flow in Power Engineering, Xi'an Jiaotong University, Xi'an 710049, China*
[2] *Bioinspired Engineering and Biomechanics Center, Xi'an Jiaotong University, Xi'an 710049, China*
[3] *The Key Laboratory of Biomedical Information Engineering of Ministry of Education, School of Life Science and Technology, Xi'an Jiaotong University, Xi'an 710049, China*

Flow behaviors of blood strongly depend on dynamics of red blood cells (RBCs) under flow. Due to the simplicity, vesicles have been extensively used as a model system to investigate RBC dynamics. Despite its significance in microfluidics, the effect of confinement (i.e., ratio of vesicle size to microchannel size) on vesicle dynamics has not been reported in three-dimensional (3D) modeling. In this study, we developed a 3D mathematical model and investigated the effect of confinement on the dynamics of oblate-shaped vesicles in microscale shear flows. Our results indicated that confinement has significant effect on the dynamics of vesicles, including tank-treading, swinging and tumbling. An increase of confinement can induce the transition of vesicle dynamics from tumbling to swinging. This study could be helpful to future studies on the flow of vesicle suspensions at microscale, e.g., *in vivo* capillaries and *in vitro* microfluidics.

Keywords: Vesicle, Dynamics, 3D Simulation, Membranes, Microscale Shear Flow, Microfluidics.

1. INTRODUCTION

Blood is primarily composed of red blood cells (RBCs) with a hematocrit (the volume fraction of RBCs) about 45% in normal human body.[1] Flow behaviors and functions of blood, e.g., mass transport, effective viscosity and flow resistance, strongly depend on the deformation and dynamics of RBCs under shear flow.[2,3] It therefore is of great importance to understand RBC dynamics and its contribution to blood rheology properties. Due to the simplicity, vesicles (a viscous fluid surrounded by a phospholipid bilayer membrane) have been extensively used as a model system to investigate RBC dynamics.[2] Besides, vesicles can also mimic the functions of biological cells in flows, holding great potential for biomedical applications, e.g., transport and delivery of drugs and containers for bioreactions. The applications of vesicles are also affected by the deformation and dynamics of vesicles.[2,4] Therefore, it is of great importance to study the dynamics of vesicles in flows.

In the last two decades, intensive analytical,[5–7] numerical[8–11] and experimental[12,13] investigations have revealed the high complexity of vesicle dynamics in flows. Even in a simple shear flow, vesicles present a variety of dynamics, e.g., tank-treading (TT), swinging (SW), tumbling (TB). In TT motion, the vesicle maintains a constant inclination angle to the flow, while vesicle membrane presents a tank-tread rotation. In SW motion, the vesicle presents TT motion except for an oscillation of the inclination angle. In TB motion, the vesicle presents a rotation like a rigid body. The dynamic states of vesicles can transit between TT, SW and TB. These transitions have been found to be affected by several factors, such as the viscosity contrast of inner and outer fluids, the initial shape of vesicles, the mechanical properties of vesicle membrane and the shear rate of surrounding shear flow. Due to the inherent complexity of vesicle dynamics, simplification and assumption have been employed in theoretical modeling, and the mechanisms of vesicle dynamics are not well known yet.

One of the main assumptions in previous studies is assuming no wall effect so that the unbound shear flow can be employed to study vesicle dynamics.[5–11] However, this assumption may not be valid especially when the flow is confined to scales comparable to vesicle sizes, for example, vesicle suspensions in microfluidics and

*Author to whom correspondence should be addressed.

blood flow in capillaries. In previous studies on vesicle deformation, the confinement (ratio of the vesicle radius to the distance between walls) was set to less than 0.1 to exclude the wall effect,[10, 11, 14] while it may be much higher to approach 0.5 in microfluidics or human microcirculatory system.[1, 15] In this case, the confinement may significantly affect tank-treading and tumbling of vesicles and can induce a transition of tumbling to tank-treading, which was demonstrated in two-dimensional (2D) numerical studies.[16, 17] However, a three-dimensional (3D) model is still in unmet need to better understand the wall effect on vesicle dynamics, as vesicles may present much different dynamic behaviors in 3D.

Here, we developed a 3D model and investigated the dynamics of vesicles in microscale shear flows. The effect of walls on vesicle dynamics was presented by varying the confinement from 0.125–0.333. Our results showed that with increasing confinement the vesicle dynamic state can transit from tumbling to swinging and the oscillation amplitude of vesicle deformation and orientation significantly decreased.

2. MODEL AND METHODS

3D numerical simulations are presented on the dynamic behaviors of an oblate-shaped vesicle in a linear shear flow (Fig. 1). To investigate the effect of confinement on vesicle dynamics, the linear shear flow is bounded by two walls with a distance of H_c. The initial velocity profile of the linear shear flow is $\mathbf{u}_0 = [\gamma z, 0, 0]$, where γ is the shear rate. The vesicle is composed of an elastic membrane enclosing a viscous fluid. Using the front tracking method, the vesicle membrane is discretized into a set of triangular elements, thus the finite element method can be used to calculate stresses in the membrane. The fluid inside and outside the vesicle is Newtonian and incompressible with viscosities $\lambda\mu_0$ and μ_0, where λ is the viscosity ratio. The flow is governed by:

$$\nabla \cdot \boldsymbol{u} = 0 \tag{1}$$

$$\rho\left[\frac{\partial \boldsymbol{u}}{\partial t} + \boldsymbol{u}\cdot\nabla\boldsymbol{u}\right] = -\nabla p + \nabla\cdot[\mu(\nabla\boldsymbol{u} + \nabla^T\boldsymbol{u})] + \int_S \boldsymbol{f}_m(\boldsymbol{x}')\delta(\boldsymbol{x}-\boldsymbol{x}')d\boldsymbol{x}' \tag{2}$$

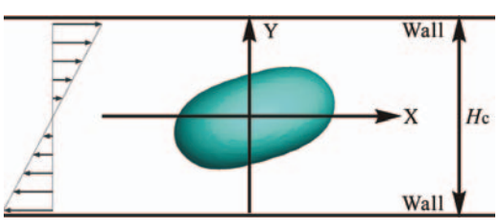

Figure 1. Schematic illustration of problem statement. A vesicle composed of an elastic membrane enclosing a viscous fluid was suspending in a linear shear flow bounded by two walls with a distance of H_c. The dynamics of the vesicle in a confined channel was simulated and the effect of confinement was investigated.

where p is the pressure, ρ the density and μ the viscosity of the fluid. $\boldsymbol{f}_\mathbf{m}$ is the membrane stress due to the resistance against shear, bending and area dilatation of vesicle membrane. The membrane stresses are transferred from Lagrangian grids onto Eulerian grids by the Dirac-Delta function δ.

The membrane stresses are determined by the deformation of the membrane. The strain-energy function by Skalak et al.[18] is employed to compute the stresses due to the resistance against shear and area dilatation:

$$W = \frac{E_s}{8}(\lambda_1^4 + \lambda_2^4 - 2\lambda_1^2 - 2\lambda_2^2 + 2) + \frac{E_a}{8}(\lambda_1^2\lambda_2^2 - 1)^2 \tag{3}$$

where λ_1 and λ_2 are principle stretch ratios, E_a and E_s are the moduli of area-dilatation and shear. The principal stresses are:

$$\begin{aligned}\tau_1 &= \frac{1}{\lambda_2}\frac{\partial W}{\partial \lambda_1} \\ &= \frac{1}{2\lambda_1\lambda_2}[E_s\lambda_1^2(\lambda_1^2-1) + E_a\lambda_1^2\lambda_2^2(\lambda_1^2\lambda_2^2-1)] \\ \tau_2 &= \frac{1}{\lambda_1}\frac{\partial W}{\partial \lambda_2} \\ &= \frac{1}{2\lambda_1\lambda_2}[E_s\lambda_2^2(\lambda_1^2-1) + E_a\lambda_1^2\lambda_2^2(\lambda_1^2\lambda_2^2-1)]\end{aligned} \tag{4}$$

The stresses in the membrane are obtained from the principal stresses and the membrane deformation. The resistance against bending is modeled using the Helfrich's bending energy function:[19, 20]

$$W_b = \frac{E_b}{2}\int_S (2H - C_0)^2 dS + E_g\int_S \kappa_g dS \tag{5}$$

where C_0 is the spontaneous curvature, E_g and E_b are the bending moduli associated with Gaussian curvature κ_g and Mean curvature H. The membrane stresses due to bending resistance are obtained by:

$$\boldsymbol{f}_b = -E_b[(2H - C_0)(2H^2 - 2\kappa_g + C_0 H) + 2\Delta_s H]\boldsymbol{n} \tag{6}$$

where $\boldsymbol{n}$ is the unit normal vector directing outward, and Δ_s is the Laplace-Beltrami operator.

Dimensionless parameters used in our model include Reynolds number $\mathrm{Re} = \rho\gamma R^2/\mu$ (R is the vesicle radius), Viscosity ratio λ, Capillary number $\mathrm{Ca} = \gamma\mu R/E_s$, Confinement $\mathrm{Cn} = R/H_c$, Dimensionless bending modulus $E_B^* = E_b/(R^2E_s)$ and Reduced volume $\chi = [V/(4\pi/3)]/(A/4\pi)^{3/2}$, where V and A are the volume and surface-area. Vesicle dynamics are characterized by two parameters: (i) deformation index $D = (L-B)/(L+B)$, where L and B are major and minor axis of the elliptical vesicle in the shear plane; (ii) inclination angle θ between the major axis of the elliptical vesicle and flow direction. To focus on the effect of confinement on vesicle dynamics, we fixed $\mathrm{Re} = 0.1$, $E_B^* = 0.05$ and $\mathrm{Ca} = 0.05$.

We used a three-stage RKCN four-step projection method with second-order temporal accuracy to solve the

governing equations. The spatial accuracy was ensured to be second order by using the standard central difference scheme. The convective and pressure terms were updated using the three-stage complete Runge-Kutta technique and the diffusion term was updated using the Crank-Nicholson semi-implicit technique. The solver was written in FORTRAN. To validate our model, we simulated the deformation of a spherical vesicle in a linear shear flow. Our model gave a deformation index and inclination angle of a vesicle without bending resistance identical to Ramanujan et al.[21] within 4.6% and 3.8%. For a vesicle with bending resistance, the discrepancy of deformation index between our prediction and Pozrikidis'[22] was 1.8%. Further details and validations of our model can be found in our previous studies.[10, 11, 23, 24]

3. RESULTS AND DISCUSSION

To investigate the effect of reduced volume on vesicle dynamics in a confined channel, we simulated the dynamic behaviors of vesicles with $\chi = 0.872 - 1$ at $\mathrm{Cn} = 1/6$, Figure 2. Vesicles with $\chi = 0.872 - 1$ presented several dynamics, such as tank-treading, swinging and tumbling, Figures 2(a)–(b). A vesicle with $\chi = 1$ exhibited a steady tank-treading motion, which assumed a steady deformation index and inclination angle. Vesicles with $\chi < 1$ presented unsteady dynamics, which assumed an oscillating deformation index and inclination angle. The swinging motion was observed for vesicles with $\chi = 0.965$ and 0.997, as the oscillation amplitude of inclination angle $\Delta\theta$ was less than π. $\Delta\theta$ increased to π as χ was decreased to 0.872, and the vesicle exhibited a tumbling motion. For vesicles with $\lambda = 1$ and 10, the equilibrium deformation index D_e linearly decreased with increasing χ, and the equilibrium inclination angle θ_e linearly increased with increasing χ, Figure 2(c). The same qualitative tendency was observed in 2D confined channels.[17] As χ was increased from 0.872–1, the oscillation amplitude of both deformation index and inclination angle rapidly decreased to 0, Figure 2(d). Vesicles under unbounded shear flows showed the same qualitative tendency.[25]

To investigate the effect of confinement on vesicle dynamics, we simulated the dynamic behaviors of a vesicle with $\chi = 0.872$ and $\lambda = 10$ in confined channels with two different confinements $\mathrm{Cn} = 1/6$ and 1/3, Figure 3. An increase of the confinement triggered a transition of vesicle dynamics from tumbling to swinging. For instance, the vesicle at $\mathrm{Cn} = 1/6$ exhibited a tumbling motion (Fig. 3(a)). The major axis of the ellipsoidal vesicle (arrows in Fig. 3(a)) rotated about the vesicle center. While Cn was increased to 1/3, the dynamic state of the vesicle was changed to a swinging motion, Figure 3(b). The major axis of the ellipsoidal vesicle (arrows in Fig. 3(b)) exhibited a swing instead of a rotation about the vesicle center. In the meantime, the vesicle membrane showed a rotation like a tank tread, which was indicated by the trajectory of a fixed

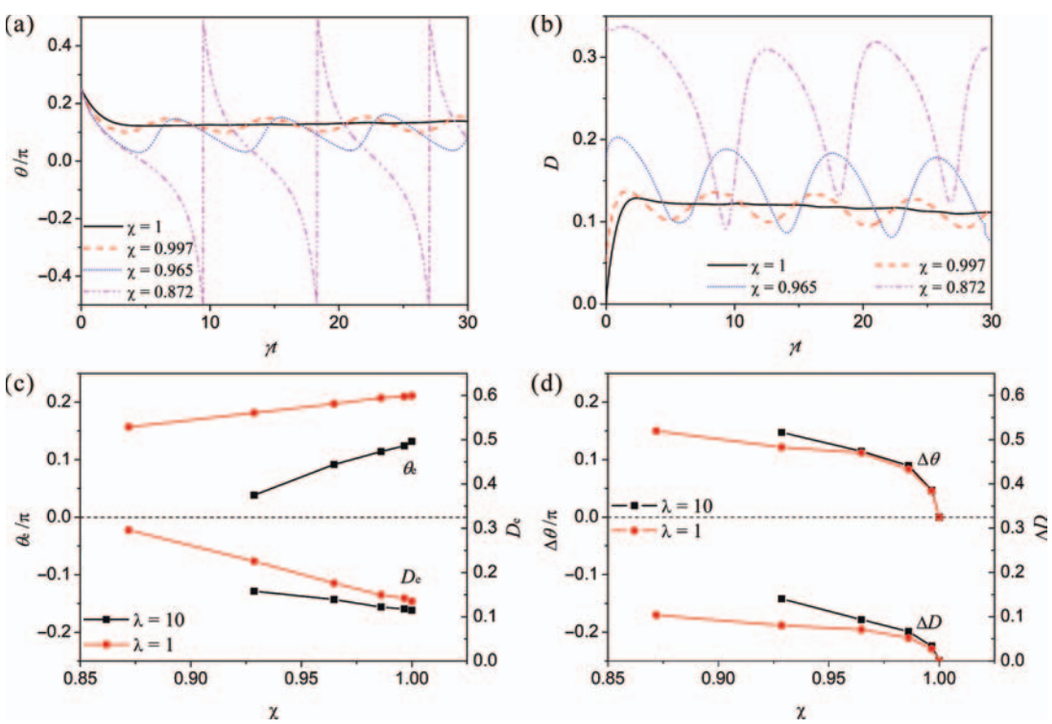

Figure 2. Dynamic behaviors of vesicles in a confined channel at $\mathrm{Cn} = 1/6$. Deformation index D (a) and inclination angle θ (b) at $\lambda = 10$ versus time γt. (c) Equilibrium inclination angle θ_e and equilibrium deformation index D_e versus reduced volume χ. (d) Oscillation amplitude of inclination angle $\Delta\theta$ and deformation index ΔD versus reduced volume χ.

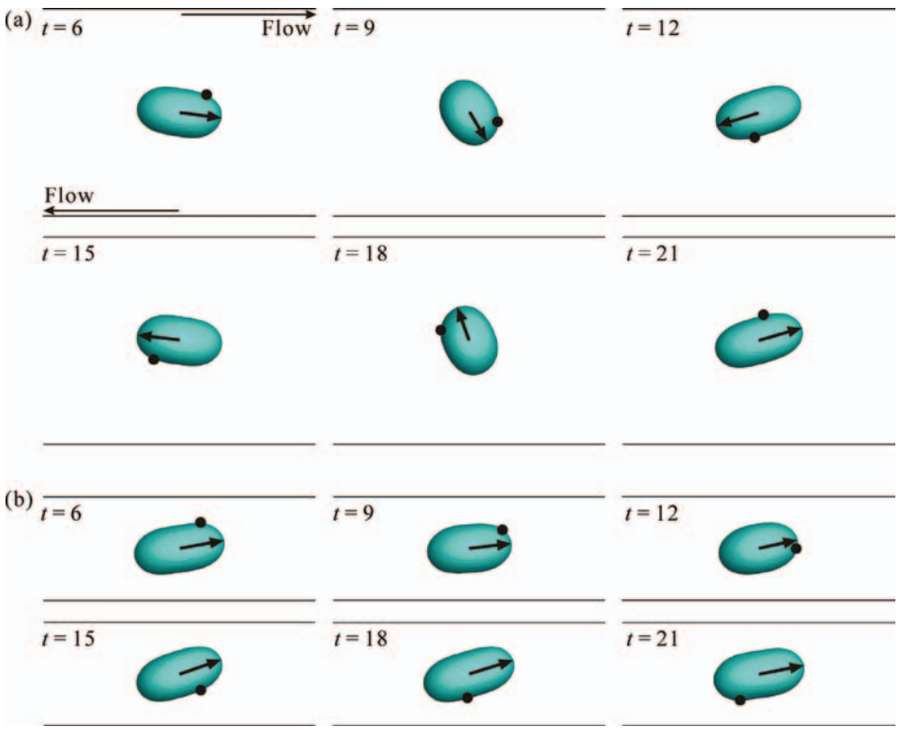

Figure 3. Different dynamic states of a vesicle with $\chi = 0.872$ and $\lambda = 10$ in two different confined channels. (a) Tumbling at $\mathrm{Cn} = 1/6$. (b) Swinging at $\mathrm{Cn} = 1/3$. Arrows indicate the major-axis of the vesicles. Black dots show the trajectory of a fixed point on vesicle membrane.

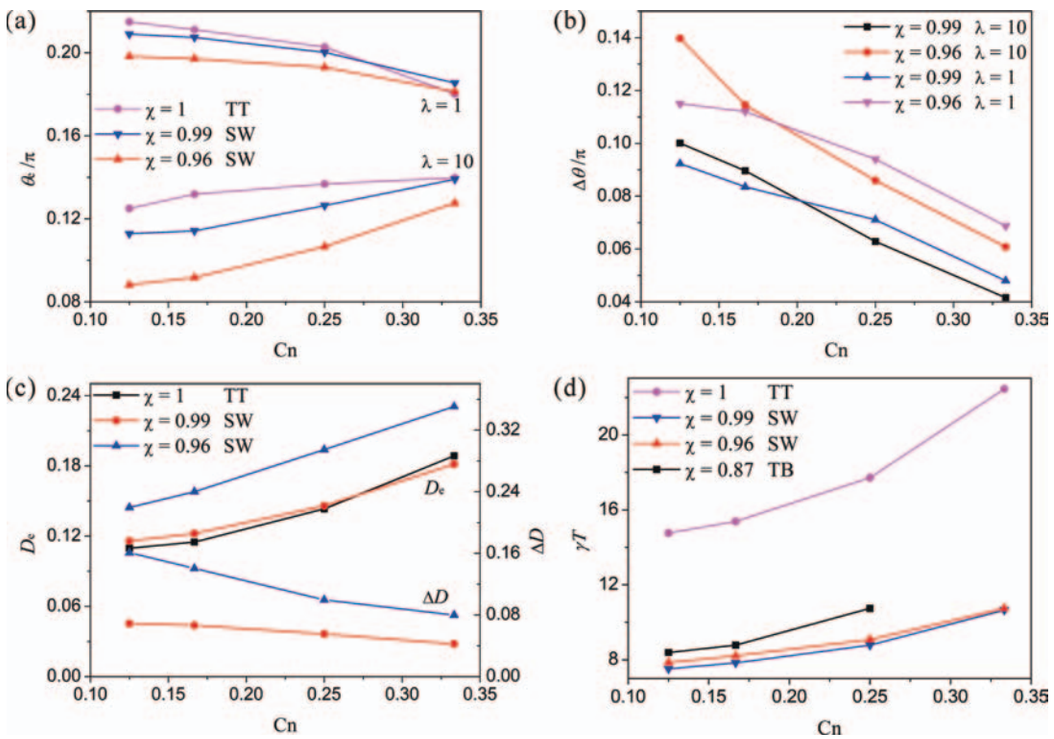

Figure 4. The effect of confinement on quantities associated to different vesicle dynamics including tank-treading, swinging and tumbling. (a) Equilibrium inclination angle versus the confinement. (b) Oscillation amplitude of inclination angle versus the confinement. (c) Equilibrium deformation index and oscillation amplitude of deformation index versus the confinement for a vesicle with $\lambda = 10$. (d) Oscillation period versus the confinement for a vesicle with $\lambda = 10$.

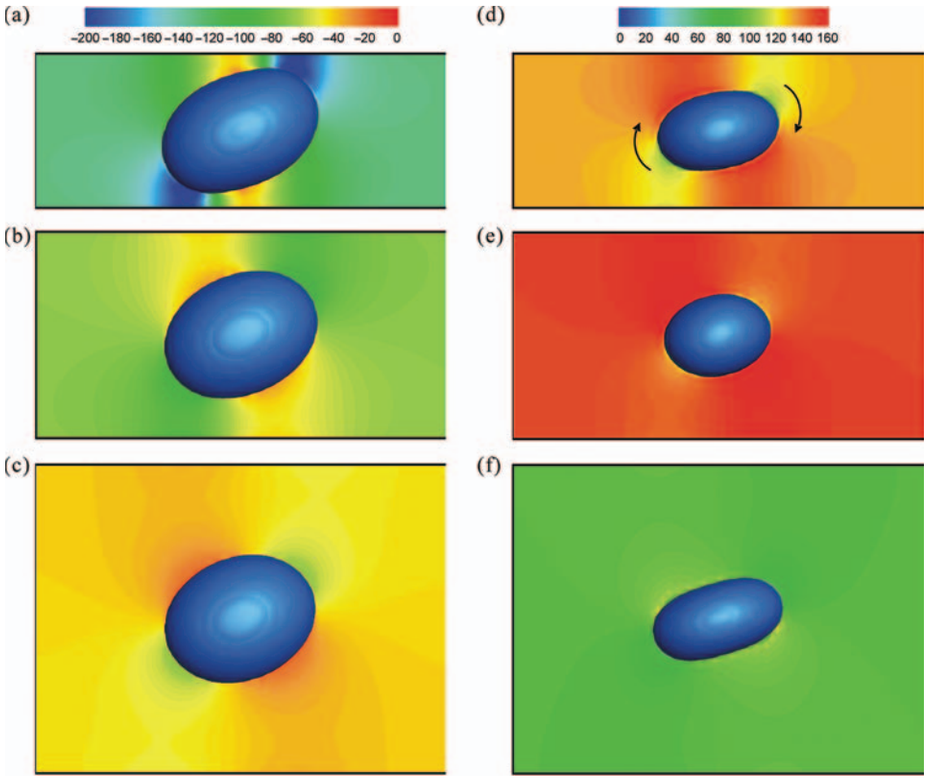

Figure 5. Pressure field outside the vesicle with $\lambda = 10$. Vesicles with $\chi = 1$ in confined channels with different values of the confinement at $\gamma t = 9$: (a) Cn = 1/3, (b) Cn = 1/4 and (c) Cn = 1/6. Vesicles with $\chi = 0.872$ in confined channels with different values of the confinement at $\gamma t = 12$: (d) Cn = 1/3, (e) Cn = 1/4 and (f) Cn = 1/6. Vesicles in (a)–(c) are in tank-treading regime; vesicle in (d) is in swinging regime and vesicles in (e) and (f) are in tumbling regime.

point on the membrane, Figure 3(b). The transition of tumbling to swinging induced by the increase of the confinement was not presented in previous 2D simulations.[16, 17]

Figure 4 showed the effect of confinement Cn on quantities associated to different vesicle dynamics of tank-treading, swinging and tumbling. Among these quantities were the equilibrium inclination angle (θ_e), the equilibrium deformation index (D_e), the oscillation amplitude (ΔD and $\Delta\theta$) and period (T) of deformation index and inclination angle. As Cn was increased from 1/8 to 1/3, θ_e monotonically decreased at $\lambda = 1$ while monotonically increased at $\lambda = 10$, no matter vesicles are in tank-treading or swinging regime, Figure 4(a). The same qualitative tendency was observed for 2D vesicles.[16] D_e monotonically increased with increasing Cn for vesicles with $\lambda = 10$, Figure 4(c). Both $\Delta\theta$ and ΔD monotonically decreased with increasing Cn for vesicles with $\lambda = 1$ and 10, Figures 4(b)–(c). The increase of the confinement suppressed the oscillations in the deformation and inclination of vesicles under shear flows. Additionally, the oscillation period T of inclination angle was observed to monotonically increase with increasing confinement for vesicles in tank-treading, swinging or tumbling regime. Here, T for vesicles in tank-treading regime represented the period of membrane tank-treading. These results indicate that the channel walls significantly affected the characteristics of vesicle dynamics, including tank-treading, swinging or tumbling, especially at high confinement.

To gain further insight of the effect of confinement on vesicle dynamics, we presented the pressure field of the shear plane in confined channels with three different confinements, Cn = 1/3, 1/4 and 1/6, Figure 5. The pressure values were relative deviations from the pressure at the center point of the vesicle. Red and blue color showed the regions with higher and lower pressure, respectively. For vesicles in tank-treading regime, an increase of the confinement induced an increase in the nonuniformity of the pressure around the vesicle, Figures 5(a)–(c), thus the deformation of vesicles increased with increasing confinement, Figure 4(c). For vesicles in tumbling regime at lower confinement Cn = 1/6 and 1/4, the pressure had no significant change along the vesicle membrane so that the pressure had no significant effect on the tumbling of vesicles, Figures 5(e)–(f). The nonuniformity of the pressure around the vesicle membrane significantly increased with increasing confinement, Figures 5(d)–(f). As the confinement was increased to 1/3, a higher pressure region was observed between the wall and the vesicle tip approaching

the wall, while a lower pressure region was observed between the wall and the vesicle tip departing from the wall, Figure 5(d). This pressure distribution caused a negative torque against the rotation or swinging of the vesicle. Thus, the oscillation amplitude of inclination angle decreased with increasing confinement, Figures 4(b)–(c), and the increase of the confinement even triggered a transition of vesicle dynamics from tumbling to swinging, Figure 3.

In summary, a 3D theoretical model was developed to study the dynamics of vesicles in a bounded shear flow. The size effect in microscale flow was presented by the effect of confinement, i.e., ratio of vesicle size to microchannel size. We found that the oscillation of vesicle deformation degree significantly decreased with increasing confinement. The dynamical state of vesicles can be alternated by increasing the confinement due to the change of pressure field resulting from the interactions between the vesicle and walls. In addition, our 3D model demonstrated that an increase in confinement can trigger the dynamical state of a non-spherical vesicle from tumbling to swinging, whilst it was from tumbling to tank-treading in previous 2D simulations.[16, 17] Therefore, our 3D model provides new insights into the effect of confinement on vesicle dynamics and can be used to further study vesicle dynamics in microscale shear flows.

4. CONCLUSION

In this paper, we developed a 3D model based on the front tracking method and investigated the dynamics of a vesicle in a confined microscale shear flow. Our results demonstrate that vesicle dynamics in confined microchannels had significant difference from that in unbound shear flows. The increase of the confinement (ratio of the vesicle size to microchannel size) significantly reduced the oscillation amplitude of deformation index and inclination angle. The oscillation period of inclination angle significantly increased with increasing confinement for vesicles in tank-treading, swinging or tumbling regime. Furthermore, an increase of the confinement can trigger a transition of vesicle dynamics from tumbling to swinging. We also explained the effect of confinement on vesicle dynamics via the change of pressure field due to varied confinements. This study provides new insight into vesicle dynamics under bounded shear flows and could be useful to study the flow of vesicle suspensions at microscale, e.g., *in vivo* capillaries and *in vitro* microfluidics.

Acknowledgments: This work was supported by the Specialized Research Fund for the Doctoral Program of Higher Education of China (20110201110029). This research was partially supported by the Foundation for Innovative Research Groups of the National Natural Science Foundation of China (Grant No. 51121092), the Major International Joint Research Program of China (11120101002), and the Key (Key grant) Project of Chinese Ministry of Education (313045).

References and Notes

1. A. S. Popel and P. C. Johnson, *Annu. Rev. Fluid Mech.* 37, 43 (**2005**).
2. P. M. Vlahovska, T. Podgorski, and C. Misbah, *C. R. Phys.* 10, 775 (**2009**).
3. J. D. Wan, A. M. Forsyth, and H. A. Stone, *Integr. Biol.* 3, 972 (**2011**).
4. M. Abkarian and A. Viallat, *Soft Matter.* 4, 653 (**2008**).
5. S. R. Keller and R. Skalak, *J. Fluid Mech.* 120, 27 (**1982**).
6. C. Misbah, *Phys. Rev. Lett.* 96, 028104 (**2006**).
7. J. M. Skotheim and T. W. Secomb, *Phys. Rev. Lett.* 98, 078301 (**2007**).
8. H. Noguchi and G. Gompper, *Phys. Rev. Lett.* 98, 188302 (**2007**).
9. T. Biben, A. Farutin, and C. Misbah, *Phys. Rev. E* 83, 031921 (**2011**).
10. B. F. Bai, Z. Y. Luo, S. Q. Wang, L. He, T. J. Lu, and F. Xu, *Microfluid. Nanofluid.* 14, 817 (**2013**).
11. Z. Y. Luo, S. Q. Wang, L. He, F. Xu, and B. F. Bai, *Soft Matter.* 9, 9651 (**2013**).
12. V. Kantsler and V. Steinberg, *Phys. Rev. Lett.* 96, 036001 (**2006**).
13. J. Deschamps, V. Kantsler, and V. Steinberg, *Phys. Rev. Lett.* 102, 118105 (**2009**).
14. X. Y. Li and K. Sarkar, *J. Comput. Phys.* 227, 4998 (**2008**).
15. J. P. Shelby, J. White, K. Ganesan, P. K. Rathod, and D. T. Chiu, *P. Natl. Acad. Sci. U.S.A* 100, 14618 (**2003**).
16. B. Kaoui, T. Kruger, and J. Harting, *Soft Matter.* 8, 9246 (**2012**).
17. B. Kaoui, J. Harting, and C. Misbah, *Phys. Rev. E* 83, 066319 (**2011**).
18. R. Skalak, A. Tozeren, R. P. Zarda, and S. Chien, *Biophys. J.* 13, 245 (**1973**).
19. W. Helfrich and Z. Naturforsch, *C. C* 28, 693 (**1973**).
20. O. Y. Zhongcan and W. Helfrich, *Phys. Rev. A* 39, 5280 (**1989**).
21. S. Ramanujan and C. Pozrikidis, *J. Fluid Mech.* 361, 117 (**1998**).
22. C. Pozrikidis, *J. Fluid Mech.* 440, 269 (**2001**).
23. B. F. Bai, Z. Y. Luo, T. J. Lu, and F. Xu, *J. Mech. Med. Biol.* 13, 1350002 (**2013**).
24. Z. Y. Luo, S. Q. Wang, L. He, T. J. Lu, F. Xu, and B. F. Bai, *Chem. Eng. Sci.* 97, 394 (**2013**).
25. J. Beaucourt, F. Rioual, T. Seon, T. Biben, and C. Misbah, *Phys. Rev. E* 69, 17 (**2004**).

Received: 21 September 2013. Accepted: 18 January 2014.